---Supporting Information---

Two-Step Coupled Photoelectrochemical Chlorination and Oxygenation of C(sp^3)-H Bonds Mediated by Chlorine Radicals over a Modified $BiVO_4$ Photoanode

Weijian Yang,[a] Pengju Li,[a] Yiming Han,[a] Zijian Zhao,[a] Limei Tian,[a] Zhenghao Zhang,[a] Mark G. Humphrey,[c] Chi Zhang,[b,*] and Ke Hu[a,b,*]

[a]Department of Chemistry and Shanghai Key Laboratory of Molecular Catalysis and Innovative Materials, Fudan University, 220 Handan Road, Shanghai 200433, P. R. China

[b]School of Chemical Science and Engineering, Tongji University, 1239 Siping Road, Shanghai 200092, P. R. China

[c]Research School of Chemistry, Australian National University, Canberra, ACT 2601, Australia

*Correspondence to chizhang@tongji.edu.cn; khu@tongji.edu.cn; khu@fudan.edu.cn

Contents

Experimental Section

Materials. Cyclohexane, NaOH, Na_2SO_3, NaCl, $CHCl_3$, ethyl acetate, triethylamine, dimethyl sulfoxide (DMSO), CH_2Cl_2, 1,4-dioxane, toluene, nitric acid (HNO_3), hydrochloric acid (HCl), ammonium oxalate and ammonium hydroxide ($NH_3 \cdot H_2O$) were purchased from Sinopharm Chemical reagent Co., Ltd. and used without further purification. Tetrakis (dimethylamido) titanium, $Ti(NMe_2)_4$ (TDMAT, 99.999%) was purchased from APK (Shanghai) Co., Ltd. *N,N*-diethyl-*p*-phenylenediamine (DPD), vanadyl acetylacetonate [$VO(acac)_2$], 5,5-dimethyl-1-pyrroline *N*-oxide (DMPO) and Nafion were purchased from Aladdin and used without further purification. Bromobenzene, methylcyclohexane, 4-Chlorotoluene, ethylbenzene, chlorocyclohexane，tert-Butylbenzene, para-xylene, 1,2,3,4-Tetrahydronaphthalene, cycloheptane, $Bi(NO_3)_3 \cdot 5H_2O$, KI, 1,4-benzoquinone, $Ni(OAc)_2 \cdot 4H_2O$, $Co(OAc)_2 \cdot 4H_2O$, $CDCl_3$, tosyl chloride, diallylamine, 2,2,6,6-tetramethylpiperidinyl-1-oxide (TEMPO) and other reagents were purchased from Adamas and used without further purification. The fluorine-doped tin oxide (FTO) electrodes (8 Ω/sq) were purchased from Suzhou Shangyang Solar Technology Co. Ltd. Prior to the electrochemical experiments, the FTO plates were cleaned by ultrasonication in deionized water, isopropanol, and ethanol (20 min), respectively.

Fabrication of $BiVO_4$. $BiVO_4$ photoanodes were obtained according to a previous report with minor modification by thermal conversion of BiOI to $BiVO_4$.[1] A 0.04 M Bi $(NO_3)_3$ solution was prepared by dissolving $Bi(NO_3)_3 \cdot 5H_2O$ in 50 mL of HNO_3 solution (pH = 1.7) with 0.4 M KI. This solution was mixed with 20 mL of absolute ethanol (100%) containing 0.23 M 1,4-benzoquinone and was vigorously stirred for a few minutes. A typical three-electrode cell with a 1×2 cm^2 FTO working electrode (WE), an Ag/AgCl (saturated KCl) reference electrode (RE), and a platinum net counter electrode (CE) was used for electrodeposition. A CHI1232c potentiostat (Shanghai Chenhua Instrument Co., Ltd.) was used for electrodeposition. Cathodic deposition of BiOI films was performed potentiostatically at -0.15 V *vs* Ag/AgCl under stirring at room temperature for 5 min. The obtained BiOI film was rinsed with deionized water and dried at room temperature. 0.2 mL of a DMSO solution containing 0.4 M $VO(acac)_2$ was placed on the BiOI electrode (1× 1 cm^2) and was annealed at 450 °C (ramping rate = 2 °C/min) in air for 2 h. Excess V_2O_5 present in the $BiVO_4$ electrodes was removed by soaking them in 1 M NaOH solution for 30 min with gentle stirring. The resulting pure $BiVO_4$ electrodes were rinsed with deionized (DI) water and dried at room temperature.

Atomic Layer Deposition (ALD) of TiO_2 on Photoanode. ALD was performed using a Picosun R-200 Std instrument with TDMAT (99.999%) as the Ti precursor in a commercial reactor. TiO_2 was deposited using TDMAT and water. The reactor temperature was maintained at 150 °C. The TDMAT reservoir was kept at 75 °C. The TDMAT was pulsed into the reactor for 0.5 s and then held for 20 s before opening the pump valve and purging for 60 s. ALD coating conditions were 150 °C and 20 torr of N_2 carrier gas with a sequence of 0.5-s metal precursor dose, 20-s hold, 60-s N_2 purge, 0.02-s H_2O dose, 20-s hold, 60-s N_2 purge. The thickness for each circle is about 0.73 Å.

Deposition of $CoNi_2O_x$ Nanosheets on Photoanode. Cobalt and nickel mixed oxide catalysts with various ratios were synthesized using the hydrothermal method.[2] $Co(OAc)_2 \cdot 4H_2O$ and $Ni(OAc)_2 \cdot 4H_2O$ (2 mmol in total, with different Co/Ni ratios) were dissolved in 25 mL of DI water, and 2.5 mL of 30% $NH_3 \cdot H_2O$ was added to the solution and kept under vigorous stirring for at least

10 min. The solution was then transferred into a 50-mL autoclave and kept at 150 °C for 3 h. The precipitate was separated by centrifugation and washed several times with DI water. After drying at 80 °C overnight, the catalysts were calcined at 350 °C in air for 2 h.

To obtain the ink for drop casting, 15 mg of catalysts was dispersed into 3 mL of isopropanol and 30 μL of Nafion mixed solution under an ultrasonic bath. 50 μL of the ink was drop-cast onto a piece of 1×1 cm^2 $BiVO_4$ or $BiVO_4/TiO_2$ photoanode and heated at 80 ℃ to obtain the $BiVO_4/TiO_2/CoNi_2O_x$ photoanode.

Characterizations. The scanning electron microscopy (SEM) was studied by ZEISS Gemini SEM 500 field-emission scanning electron microscope. High-resolution transmission electron microscopy (HRTEM), and scanning transmission electron microscopy energy dispersive X-ray spectroscopy (STEM-EDS) elemental mapping were carried out with a FEI Tecnai G2 F20 microscope. The X-ray photoelectron spectroscopy (XPS) spectra were collected by PHI5300. The X-ray diffraction (XRD) was carried out with a Bruker D2 PHASER.

Photoelectrochemical (PEC) Characterizations. Linear sweep voltammetry (LSV) and photocurrent density *vs* time (*J*-t) tests were performed in a three-electrode electrochemical cell using a CHI 760E potentiostat (Shanghai Chenhua Instrument Co., Ltd.) at room temperature. In the three-electrode electrochemical system, the photoanodes served as WE, with an Ag/AgCl electrode (saturated KCl) as RE and a platinum net electrode as CE. A H-type photoelectrochemical cell (50 mL for each compartment, Gaoss Union Technology Co., Ltd.) with a quartz window was used, where the anodic and cathodic compartments were separated by Nafion 117. AM 1.5G illumination was provided by a 300 W Xe lamp (CME-303, Microenerg Beijing Technology) outfitted with an AM 1.5G filter, and the light intensity was calibrated to be 100 $mW \cdot cm^{-2}$. All photoelectrochemical measurements were conducted using backside illumination (FTO|$BiVO_4$ side). Photocurrent density *vs* applied bias (*J*–V) curves were obtained by LSV at a scan rate of 5 mV/s. All measured potentials were converted to the reversible hydrogen electrode (RHE):

$$E\ (V\ vs\ RHE)\ =\ E_{Ag/AgCl} +\ 0.197\ V\ +\ 0.0591\ V\ \times\ pH \#(1)$$

Generally, 30 mL 0.5 M NaCl solution (pH=2) was added to each compartment for the chlorine evolution reaction tests.

IPCE spectra were measured at an applied bias (E_{app}) of 1.2 V *vs* RHE on a CIMPS system equipped with ZENNIUM X potentiostats, PP212 external potentiostats, and TLS03 LED arrays (Zahner-Elektrik GmbH & Co. KG). The IPCE values were calculated as follows:

$$IPCE\ (\%)\ =\ \frac{\frac{1240}{\lambda} \times \left(J_p - J_{dark}\right)}{P} \times 100\%\ \#(2)$$

where λ is the wavelength, J_p is the photocurrent density under irradiation, J_{dark} is the current density in darkness, and P is the incident light power density.

Electrochemical impedance spectroscopy (EIS) spectra were obtained in a 0.5 M NaCl solution (pH 2) under the illumination of a TLS01 LED (white LED, Zahner-Elektrik GmbH & Co. KG, light intensity of 100 mW/cm^2) over a frequency range from 4k to 0.1 Hz at 0.8 V *vs* RHE. The resulting data were fitted using the ZView software.

Intensity Modulated Photocurrent Spectroscopy (IMPS) Measurements. IMPS measurements were conducted using a potentiostat (IM6ex, Zahner Company) controlled by a Zahner IMPS electrochemical workstation. Intensity-modulated light was provided by a TLS01 LED, which allowed the superimposition of sinusoidal modulation (~10%) at a dc illumination

level. The average intensity of the visible light was 100 mW·cm^{-2}. The photocurrent as a function of frequency (from 10 kHz to 0.1 Hz) was recorded at different potentials. The same three-electrode configuration and electrolyte were employed as described in the PEC Characterizations section.

Figure S7a shows a complex plane plot of the IMPS spectrum for various $BiVO_4$-based photoanodes at 0.8 V *vs* RHE in chlorine evolution reaction condition. In the Nyquist plot, each photoanode displayed two semicircles, corresponding to the resistance-capacitance attenuation and the competition between electron/hole transfer and carrier recombination, respectively. A calculated example of the IMPS spectrum for various kinetics properties is shown in Figure S7b. In the IMPS technique, the perturbed photocurrent $j_{photo}(\omega)$ is expressed as follows:[3]

$$\frac{j_{photo}(\omega)}{I_0} = \frac{k_{tr} + i\omega\frac{C}{C_{sc}}}{k_{tr} + k_{rec} + i\omega}\left(\frac{1}{1 + i\omega RC}\right) \#(3)$$

$$C = \frac{C_H C_{sc}}{C_H + C_{sc}} \#(4)$$

where I_0 is the periodic flux of photogenerated holes corresponding to the Gärtner equation, k_{tr} is the charge transfer rate constant, k_{rec} is the charge recombination rate constant, C is the effective capacitance, C_{SC} is the space-charge capacitance, R is the total series resistance, ω is the light modulation frequency, and C_H is the Helmholtz capacitance. Generally, the Helmholtz capacitance is much larger than space charge capacitance ($C_{sc} \ll C_H$), so I_0 approximately equals the value of the intercept at high frequency (I_2, $I_2 = I_0 C_H / (C_H + C_{sc})$). Hence, the upper semicircle can be used to determine k_{tr} and k_{rec} from the frequency at the summit (f_{max}, $2\pi f_{max} = k_{tr} + k_{rec}$) and the intercept at low frequency with the real axis I_1 [$I_1 = I_0 k_{tr} / (k_{tr} + k_{rec}) \approx I_2 k_{tr} / (k_{tr} + k_{rec})$], as shown in Figure S6b. The charge transfer efficiency (η_{ct}) value is calculated by η_{ct} (%) = $k_{tr} / (k_{tr} + k_{rec}) \times 100\%$.

Chlorine Evolution Reaction (CER) Product Analysis. The Faradaic efficiency (FE) of the CER on different photoanodes was quantified using the DPD colorimetric method. The CER performance was tested in a 30 mL 0.5 M NaCl (pH = 2) electrolyte, similar to the conditions in PEC Characterizations. Prior to the test, the electrolytic cell was sealed and purged with argon for 20 min to remove oxygen. A small bottle containing 10 mL of 2 M NaOH solution was connected to the electrolytic cell. After the CER test was completed, the electrolytic cell was purged with argon for 10 min again. Then, 1 mL of NaCl electrolyte was diluted 100 times to obtain a diluted NaCl electrolyte (solution A); 1 mL of NaOH solution was mixed with 2 mL 1 M HCl and diluted to 100 mL (solution B) for subsequent quantitative analysis. A 5 mL DPD solution (1.1 g/mL) and 5 mL phosphate buffer solution (pH = 6.8) were mixed with 100 mL solution A or solution B in a conical flask and shaken. The absorbance peak at 510 nm for the solutions were measured using a UV-Vis spectrophotometer (Agilent Cary 60) and quantitatively analyzed based on the standard curve. The standard curve was established using I_2 instead of Cl_2, as I_2 undergo a color reaction with the DPD solution according to the above steps. The concentration range of I_2 samples is 0-2.00 mg/L (converted to Cl mass). The FE of CER is calculated according to the following equation:

$$FE\ of\ CER\ (\%) = \frac{2 \times F \times (c_A \times V_A + c_B \times V_B)}{Q_{total}} \times 100\% \#(5)$$

where c_A is the concentration of Cl_2 in solution A, V_A is the volume of solution A, c_B is the concentration of Cl_2 in solution B, V_B is the volume of solution B, F is the Faraday constant, and Q_{total} is the total electric charge.

The FE of oxygen evolution reaction (OER) was determined by gas chromatography (GC) using a Gas Chromatograph 9790 Plus (Zhejiang Fuli Analytical Instruments Inc.) with a thermal conductivity detector (TCD). A 20 mL 0.5 M NaCl (pH = 2) electrolyte was used for the OER test. To remove the Cl_2 from the cell, 10 mL saturated Na_2SO_3 solution was added into the cell and shaken for 2 min. The FE of OER was calculated by assuming that all of the charges were caused by $4e^-$ oxidation of H_2O molecules to produce O_2.

PEC CER Test for 24 h on $BiVO_4/TiO_2/CoNi_2O_x$. The long time-scale (24 h) CER performance of $BiVO_4/TiO_2/CoNi_2O_x$ was tested at 0.8 V *vs* RHE in a quartz square electrolytic cell (length 6 cm × width 6 cm × height 6 cm) with 100 mL 0.5 M NaCl electrolyte (pH=2) and illuminated by white LED (100 $mW \cdot cm^{-2}$). The following FE calculation procedure was the same as CER Product Analysis.

Product Analysis for the C−H Chlorination of Cyclohexane. Generally, the photoanode was immersed in 30 mL of 0.5 M NaCl (pH = 2) solution and purged with argon gas for 20 min. Then, 2 mL of cyclohexane was added to the solution and continuously stirred at 500 rpm. Next, the PEC chlorination reaction was performed at a potential of 0.8 V *vs* RHE under AM 1.5G simulated solar light (100 $mW \cdot cm^{-2}$) for different hours at room temperature. After the reaction, 5 mL of 1 M Na_2SO_3 solution was added to remove residual chlorine, followed by extraction with 2 × 10 mL of ethyl acetate or $CHCl_3$ to obtain the organic phase product. 2.5 mL of the organic phase was taken and 10 μL of 1,4-dioxane was added as an internal standard. The organic phase product was quantified using GC (Gas Chromatograph 9790) with a flame ionization detector (FID) and the product structure was determined using gas chromatography–mass spectrometry (GC-MS) on a PE680-ST8 instrument.

Product Analysis for the C−H Chlorination of Other Organic Substrates. For the chlorination reactions of other organic substrates, the photoanode was immersed in 30 mL of 0.5 M NaCl (pH = 2) solution and purged with argon gas for 20 min. For the chlorination of methylcyclohexane, 0.2 mmol of the substrate was added to the solution. For other organic substrates, 1 mL of each substrate was added to the solution. Next, the PEC chlorination reaction was performed at a potential of 0.8 V *vs* RHE under the illumination of white LED (100 $mW \cdot cm^{-2}$, Hecho S5000 65 W LED cold light, Nanjing Hecho Technology Co., Ltd.·) and continuously stirred at 500 rpm for 2 hours at room temperature. After the reaction, 5 mL of 1 M Na_2SO_3 solution was added to remove residual chlorine, followed by extraction with 2 × 10 mL of ethyl acetate to obtain the organic phase product. The structure of the organic products was determined using GC-MS (PE680-ST8). The quantitation of chlorinated products was achieved using GC (Gas Chromatograph 9790) or a 400 MHz ^1H NMR (BRUKER, AVANCE III HD) in $CDCl_3$.

Product Analysis for the C−H Oxidation of Hydrocarbons. For the oxidation reactions of the organic substrates, the photoanode was immersed in 20 mL of 0.1 M NaCl (pH = 2) solution and purged with O_2 for 20 min. 4 mL of each organic substrate was added to the solution. Next, the PEC oxidation reaction was performed at a potential of 0.8 V *vs* RHE under the illumination of white LED (100 $mW \cdot cm^{-2}$) and continuously stirred at 500 rpm for 6 hours at room temperature. After the reaction, 5 mL of 1 M Na_2SO_3 solution was added to remove residual chlorine, followed by extraction with 2 × 10 mL of ethyl acetate to obtain the organic phase product. The quantitation

of oxygenated products was achieved by GC or ^{1}H NMR.

FE Calculation for the Main Product (FE_{main}). The FE_{main} of the reaction could be determined by the following equation:

$$FE_{main} = \frac{n \times m_{main} \times F}{Q_{total}} \times 100\% \#(6)$$

where n is the number of electrons required to generate one product molecule from one substrate molecule, m_{main} is amount of the main product (mol), F is the Faraday constant, and Q_{total} is the total electric charge. Typically, for chlorinated product n = 2, for alcohols n = 2, for aldehydes/ketones n = 4, for acid n = 6.

In the experiment examining the effect of varied irradiation wavelengths on FE, illumination is provided by a Mercury lamp (HAMAMATSU, L9588-02, light intensity of 100 mW/cm^2) with appropriate combination of filters (SP 290, LP 290 and SP 340, LP 340 and SP 380, LP 380 and SP 450, LP 450). Compared with white LED lights, mercury lamps have a smaller spot area, resulting in lower FE under the same light intensity and irradiation time.

EQE Calculation with Varied Irradiation Wavelengths. The external quantum efficiency (EQE), which represents the number of product molecules produced per incident photon by dividing the total number of products by the number of incident photons, was measured under the same reaction conditions. The illumination is provided by Mercury lamp with different filters (SP 290, LP 290 and SP 340, LP 340 and SP 380, LP 380 and SP 450, LP 450). The intensity of irradiation light was measured by using a power meter. The EQE was calculated according to the following equations.

$$EQE = \frac{N_e}{N_p} \times 100\% = \frac{M \times N_A}{N_p} \times 100\% \#(7)$$

$$N_p = \frac{P \times S \times t \times \lambda}{h \times c} \#(8)$$

Where, N_p is the total incident photons, N_e is the total reactive electrons, M is the moles of the products (chlorocyclohexane), N_A is Avogadro constant, h is the Planck constant, c is the speed of light, S is the irradiation area, P is the intensity of irradiation light, t is the photoreaction time, λ is the wavelength of the light. In this experiment, the total number of N_p in different wavelength ranges needs to be integrated and calculated.

Reaction between Cl_2 and Cyclohexane. 50 mL of 0.5 M NaCl solution (pH=2) was bubbled with Cl_2 obtained by the reaction of $KMnO_4$ and concentrated HCl for 15 min (with extreme caution). 10 mL of the obtained Cl_2-NaCl solution was transferred into a vial and mixed with 0.3 mmol cyclohexane. The vial was placed in darkness or illuminated under different conditions. The amount of chlorocyclohexane was determined by GC.

Synthesis of *N, N*-Diallyl-4-Methylbenzenesulfonamide (1a). Triethylamine (8.4 mL, 60 mmol) was added dropwise to a stirred solution of diallylamine (7.4 mL, 60 mmol) in dichloromethane (200 mL) at 0 °C. After 0.5 h, tosyl chloride (9.5 g, 50 mmol) was slowly added to the mixture. The solution was allowed to warm to room temperature and then stirred overnight. It was washed with water and brine, dried over Na_2SO_4, and concentrated on a rotary evaporator. After evaporation of the solvent, the residue was subjected to flash column chromatography (silica gel. hexane/ethyl acetate = 4/1) to give N, N-diallyl-4-methylbenzenesulfonamide (10.2 g, 81% yield). ^{1}H NMR (400 MHz, $CDCl_3$)[4] δ: 7.70 (d, J = 8.3 Hz, 2H), 7.29 (d, J = 8.3 Hz, 2H), 5.66-5.55

(m, 2H), 5.16-5.13 (m, 2H), 5.13-5.10 (m, 2H), 3.79 (d, J = 6.2 Hz, 4H), 2.42 (s, 3H) (See in Figure S28).

Setups for PEC Controlled Trials. The controlled trials were tested in a quartz square electrolytic cell (length 6 cm × width 6 cm × height 6 cm) with 60 mL of 0.5 M NaCl electrolyte (pH=2) and illuminated by a white LED (100 mW·cm^{-2}). For the chlorination of cyclohexane, 2 mL of cyclohexane was added. The PEC chlorination was conducted at 1.2 V *vs* RHE for 2 h under different photoanode placed positions (with a gap of 3 cm or no gap between the backside of the photoanode and the inner wall of the cell). When there is no gap between the photoanode and the inner wall of the cell, the outer wall of the cell was covered by the 3M black tape, leaving a window of 1 × 1 cm^2 for incident light passing. The similar test conditions for the cyclohexane chlorination here were applied on 50 μL **1a**. The analysis of its chlorinated products was according to prior reports.[4, 5]

Transient Absorption (TA) Spectroscopy. TA spectra were acquired on a TSP-2000 (Unisoku Co., Ltd.) laser flash photolysis system. Briefly, a 75 W Xenon arc lamp was served as the probe beam that focused onto the solution sample in a 10 mm cuvette. The probe beam was aligned orthogonally to the excitation laser pulse and was passed into an f/4 monochromator (Acton, Princeton Instrument) that coupled an R2949 photomultiplier tube (Hamamatsu) to achieve signal detection. A Q-switched frequency-tripled pulsed Nd:YAG laser (Quantel Q-Smart 450, 10 Hz) was used as the excitation source to output 355 nm laser pulses (5-8 nm full width at half-maximum, 10 mJ per pulse). Transient absorption kinetic data at each wavelength were acquired on a computer interfaced digital oscilloscope (LeCroy 4024, 12 bit, 200 MHz) with typical 100 laser pulse averages. For the chlorine radical detection, the TA experiment was conducted under operando condition where Cl_2 is generated from 0.5 M NaCl (pH = 2) aqueous solution in an operating PEC cell. The solution also contained 1 ml toluene for the detection of transient $Cl^{\bullet}$. For the dichloride radical detection, the saturated Cl_2-NaCl solution (0.5 M NaCl) was used for TA measurements.

Electron Spin Resonance (ESR) Measurements. ESR spectra were obtained on a Bruker EMXplus-6/1 spectrometer (300 K, 9.823 GHz, X-band). The microwave power employed was 6.325 mW. The sweep width was set to 100.0 G. The modulation frequency and modulation amplitude were 100k Hz and 1.000 GHz, respectively. To trap chlorine radical in a closely mimicked the experimental conditions way, we conducted the PEC CER in 0.5 M NaCl (pH = 2) aqueous solution with E_{app} = 0.8 V *vs* RHE and white LED irradiation. After a certain amount of Cl_2 was generated through the PEC process under the real experiment conditions, 1 ml of the reaction solution was taken and added 12 μl of 5,5-dimethyl-1-pyrroline N-oxide (DMPO) as the trapping agent for ESR testing.

Figure S1-S32

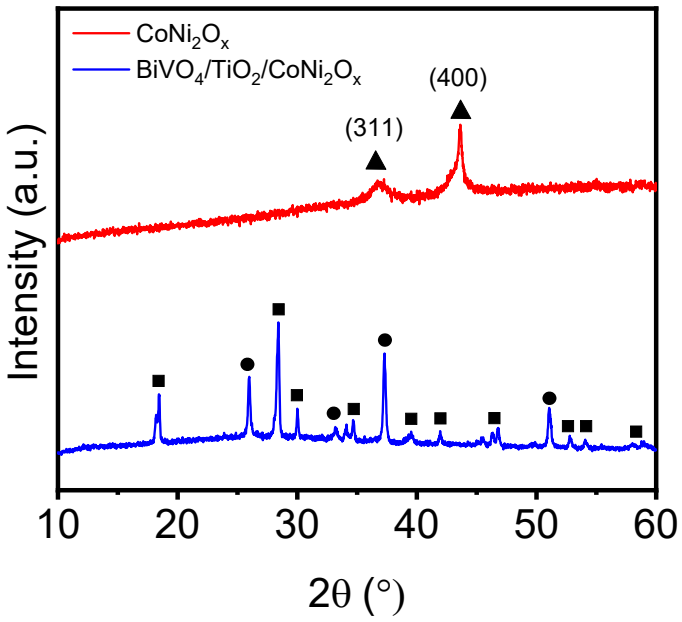

Figure S1. XRD spectra of $CoNi_2O_x$ nanosheets and $BiVO_4/TiO_2/CoNi_2O_x$. Square: monoclinic $BiVO_4$; circle: FTO; triangle: $CoNi_2O_x$.

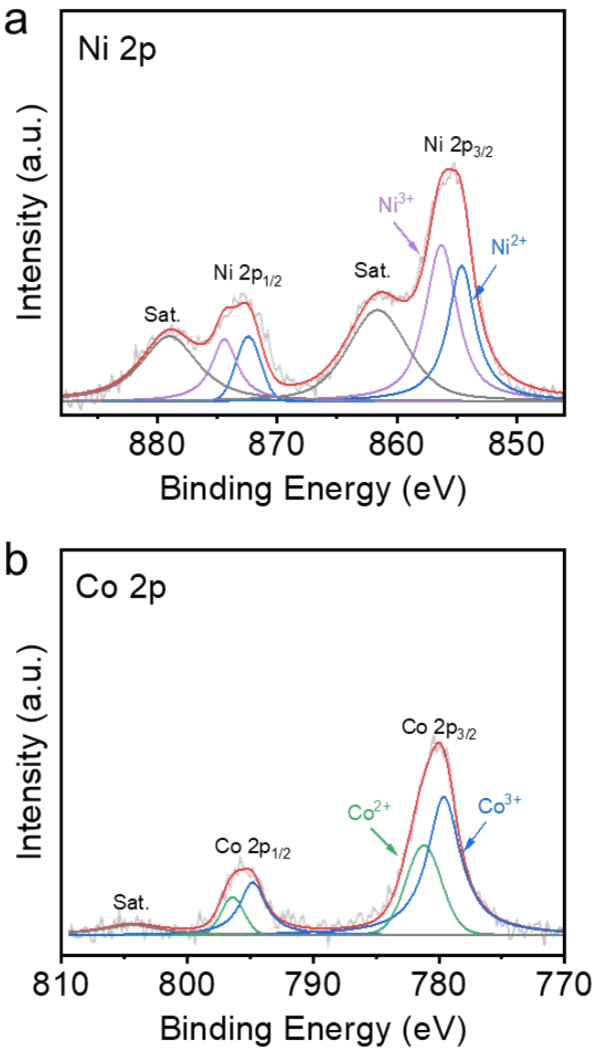

Figure S2. XPS spectra of (a) Ni 2p and (b) Co 2p for the $CoNi_2O_x$ nanosheets.

Ni 2p spectra contain spin-orbit doublets of Ni $2p_{3/2}$ and Ni $2p_{1/2}$ together with the corresponding satellite peaks (marked as "Sat."). These spin-orbit doublets can be fitted into peaks matching with the Ni^{2+} (854.6 eV and 872.4 eV) and Ni^{3+} (856.3 eV and 874.4 eV). Co 2p XPS spectra contain spin-orbit doublets of Co $2p_{3/2}$ and Co $2p_{1/2}$ together with the satellite peaks. These can also be identified with two pairs of doublet peaks, demonstrating Co^{3+} (779.6 eV and 794.8 eV) and Co^{2+} (781.2 eV and 796.4 eV).

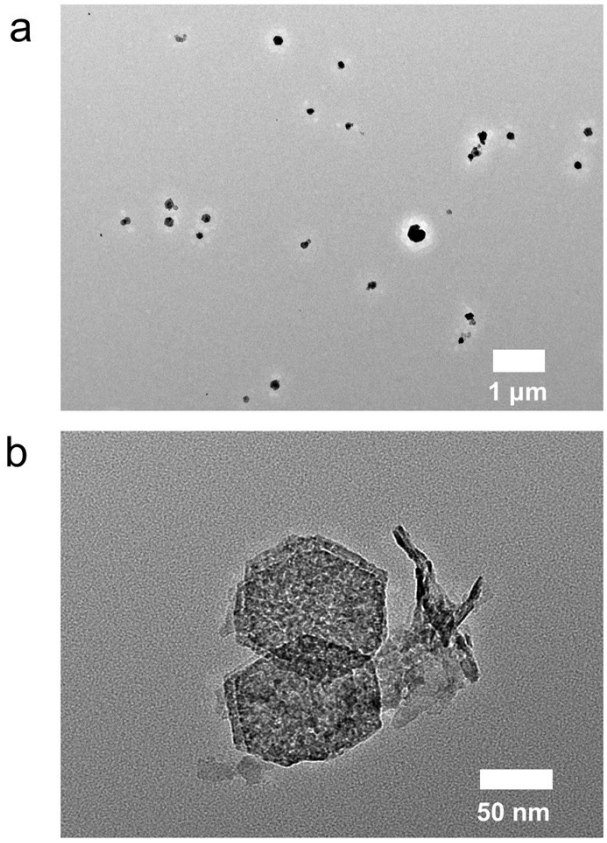

Figure S3. HRTEM images of $CoNi_2O_x$ nanosheets. Scale bar: (a) 1 μm (b) 50 nm.

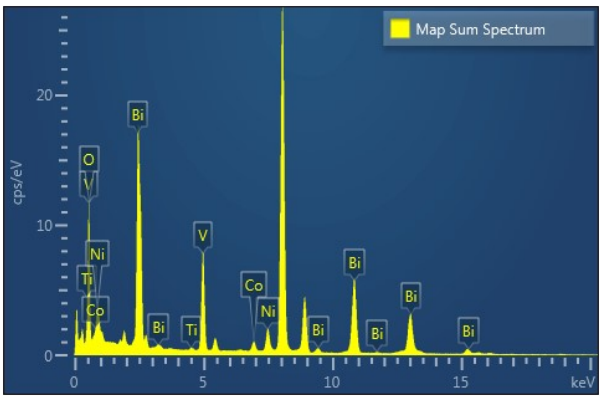

Figure S4. STEM-EDS results of $BiVO_4/TiO_2/CoNi_2O_x$.

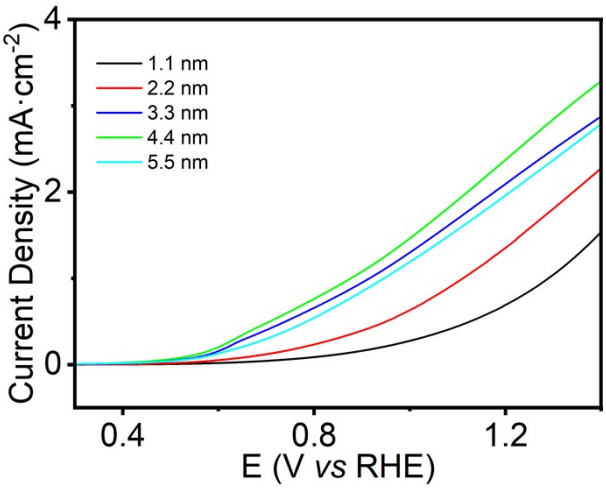

Figure S5. LSV curves of $BiVO_4/TiO_2$ photoanode with different thickness of TiO_2. Electrolyte: 0.5 M NaCl (pH = 2) solution. Illumination: AM 1.5G, 100 $mW \cdot cm^{-2}$.

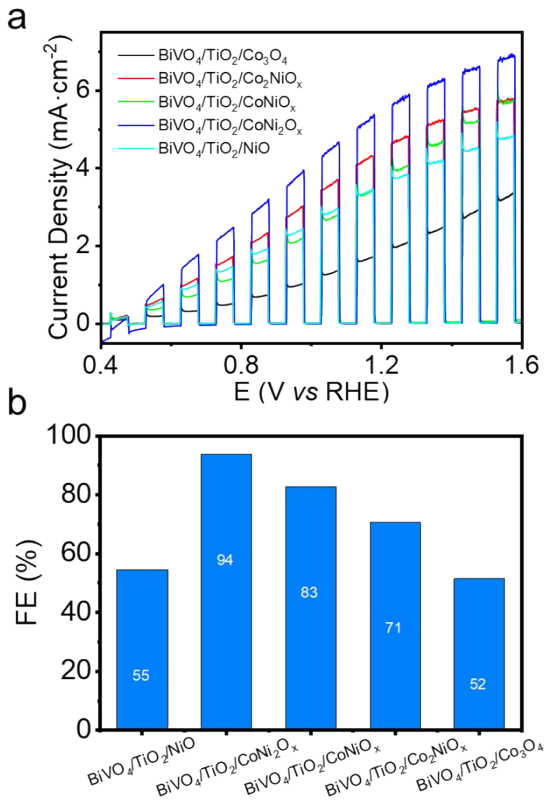

Figure S6. (a) LSV curves and (b) FE of CER in tests of 1 h for $BiVO_4/TiO_2$ based photoanode modified with different Co/Ni ratios CER catalysts.

To determine the optimized composition for the cobalt nickel oxide CER catalysts, we prepared the catalysts with different Co/Ni ratios (Co_3O_4, Co_2NiO_x, $CoNiO_x$, $CoNi_2O_x$ and NiO). Among the $BiVO_4/TiO_2$ photoanode modified with different Co/Ni CER catalysts, $BiVO_4/TiO_2/CoNi_2O_x$ displayed the highest photocurrent density and the best FE of CER compared to other photoanodes, consistent with a previously reported electrocatalytic CER result.[2] Therefore, $CoNi_2O_x$ was chosen as the optimized CER catalyst and was used hereafter.

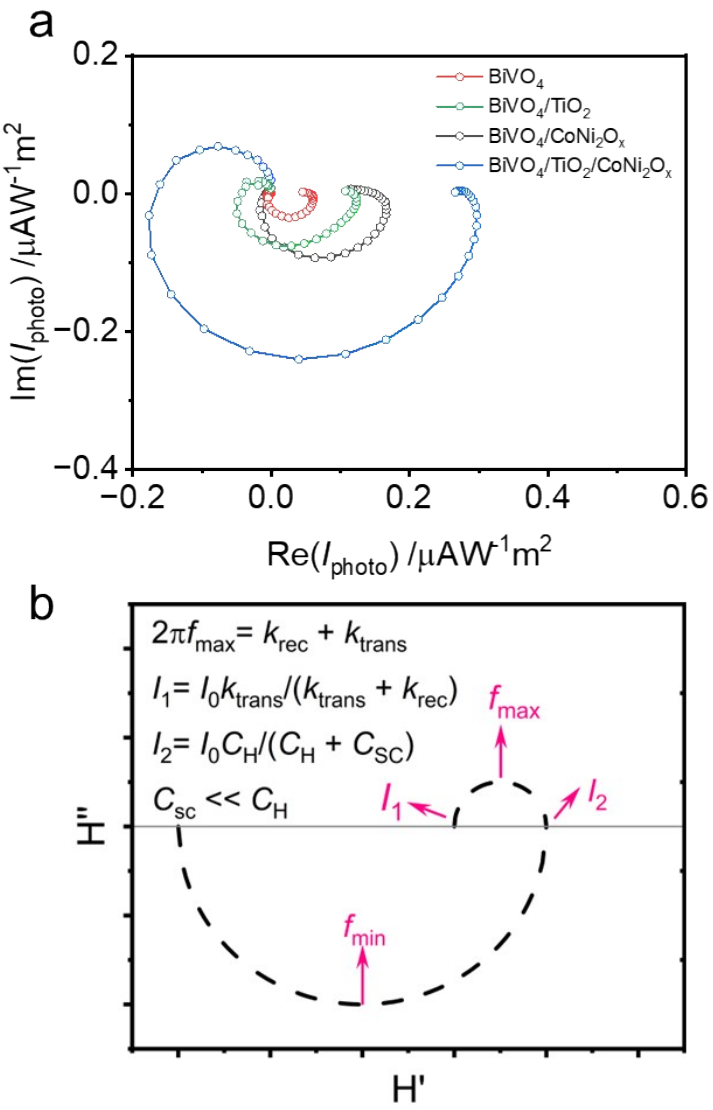

Figure S7. (a) IMPS spectra of different photoanodes at 0.8 V *vs* RHE in 0.5 M NaCl (pH = 2) solution. (b) The schematic illustration of the IMPS results.

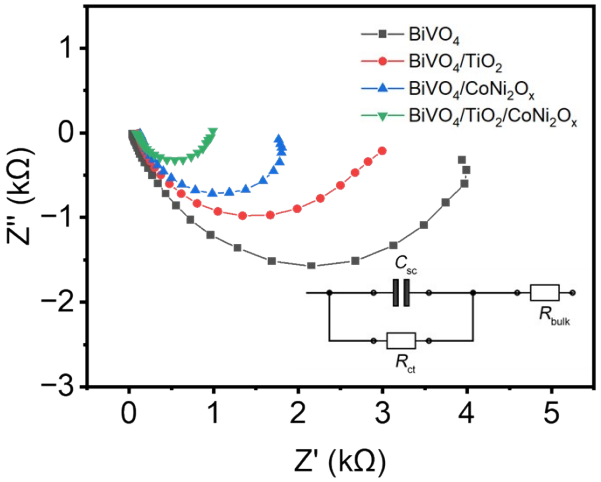

Figure S8. EIS spectra of different photoanodes collected at 0.8 V *vs* RHE in 0.5 M NaCl electrolyte (pH = 2). Insert: the Randle's equivalent circuit consisting of charge transfer resistance (R_{ct}), C_{sc}, and bulk resistance (R_{bulk}).

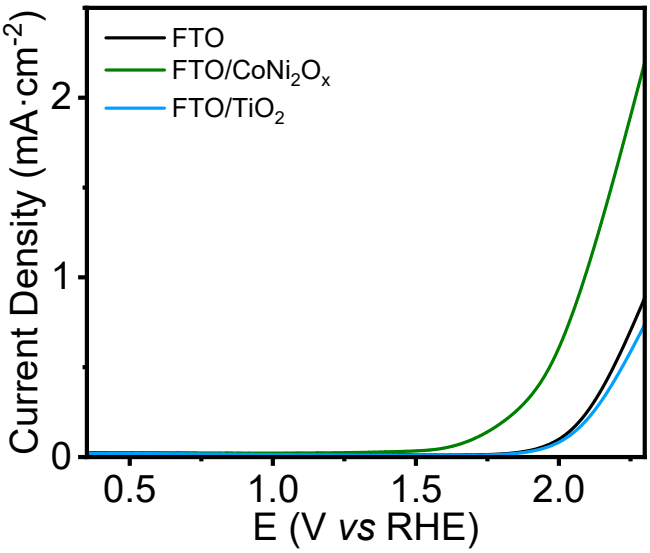

Figure S9. LSV curves of different anodes. Electrolyte: 0.5 M NaCl (pH = 2) solution.

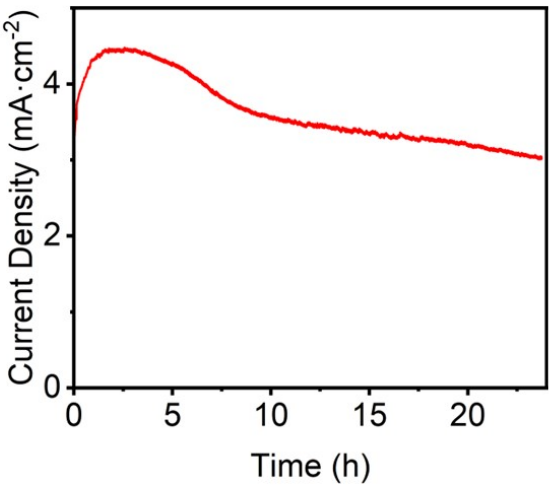

Figure S10. *J*-t curves for long-term PEC CER tests of $BiVO_4/TiO_2/CoNi_2O_x$ photoanode in 0.5 M NaCl (pH = 2) aqueous solution at 0.8 V *vs* RHE under white LED illumination. The FE of CER for $BiVO_4/TiO_2/CoNi_2O_x$ was 80% for the test of 24 h.

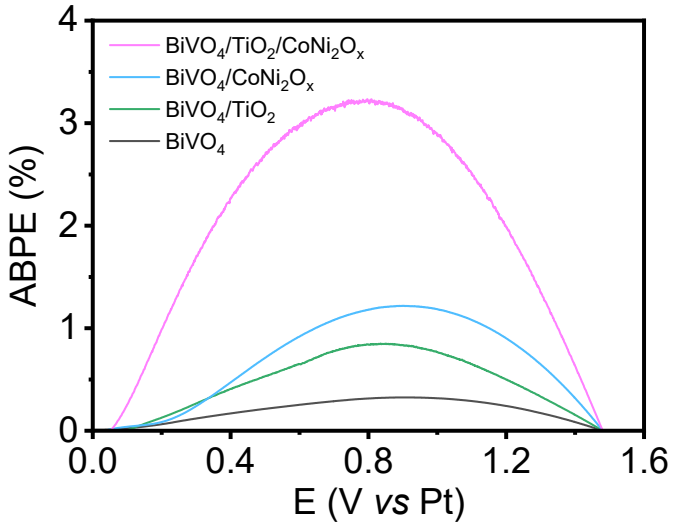

Figure S11. The applied bias photon to current efficiency (ABPE) curves of different photoanodes obtained using a two-electrode cell for PEC CER.

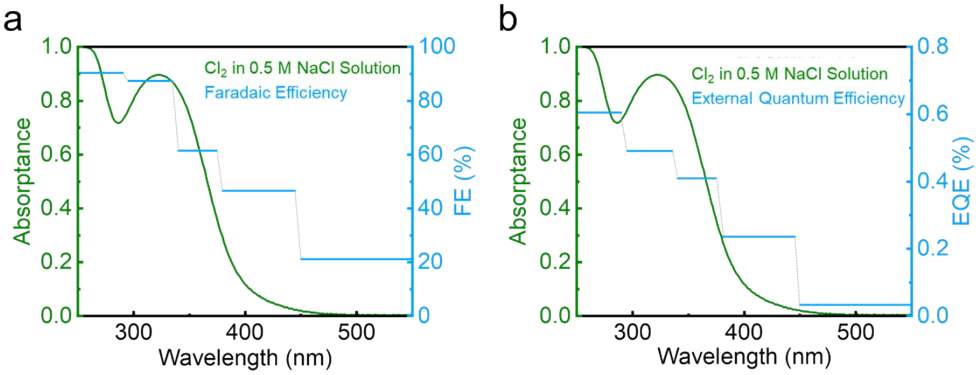

Figure S12. (a) UV-vis absorptance spectrum of Cl_2 in 0.5 M NaCl solution (left vertical axis) and FE of chlorinated products (right vertical axis) with varied irradiation wavelengths. (b) UV-vis absorptance spectrum of Cl_2 in 0.5 M NaCl (pH = 2) aqueous solution (left vertical axis) and EQE of Cl_2 to product per incident photon (right vertical axis). Absorptance = $1\text{-}10^{\text{-Abs}}$.

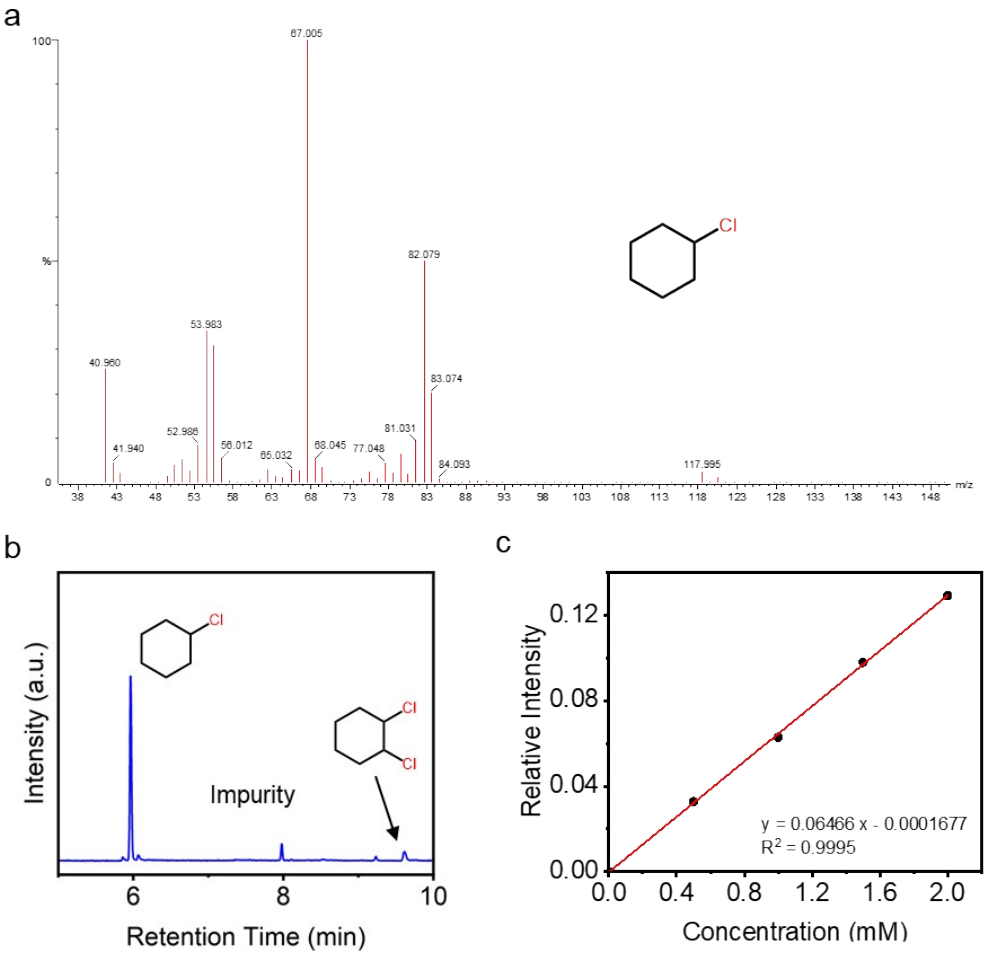

Figure S13. (a) MS spectrum of main product for the chlorination of cyclohexane. (b) GC spectrum of the chlorination products for cyclohexane. (c) The standard curves of chlorocyclohexane for quantitation by GC.

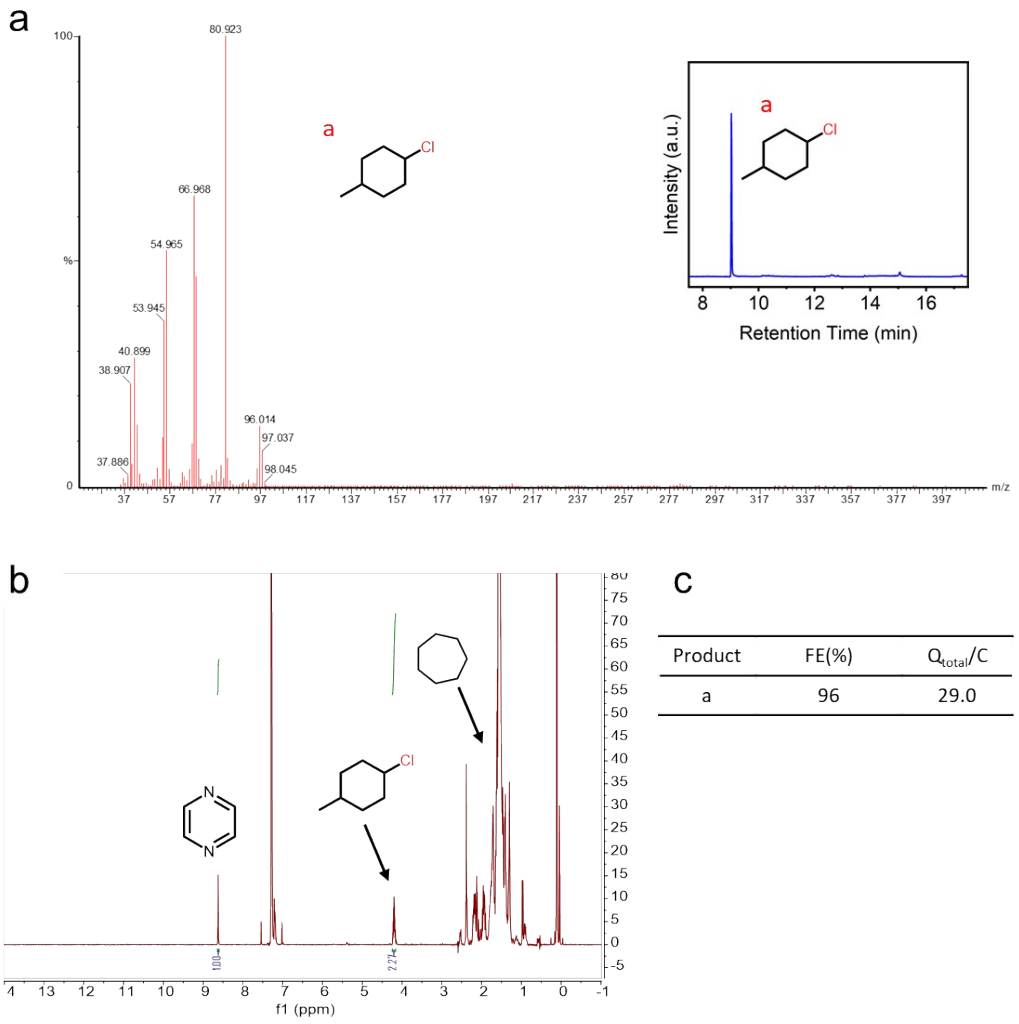

Product	FE(%)	Q_{total}/C
a	96	29.0

Figure S14. (a) MS spectrum of the main chlorination product for cycloheptane. Insert: GC spectrum of the chlorination products for cycloheptane. (b) ^{1}H NMR spectrum of the chlorination products with 16 μmol pyrazine as internal standard in $CDCl_3$. (c) The calculated FE of the reaction product.

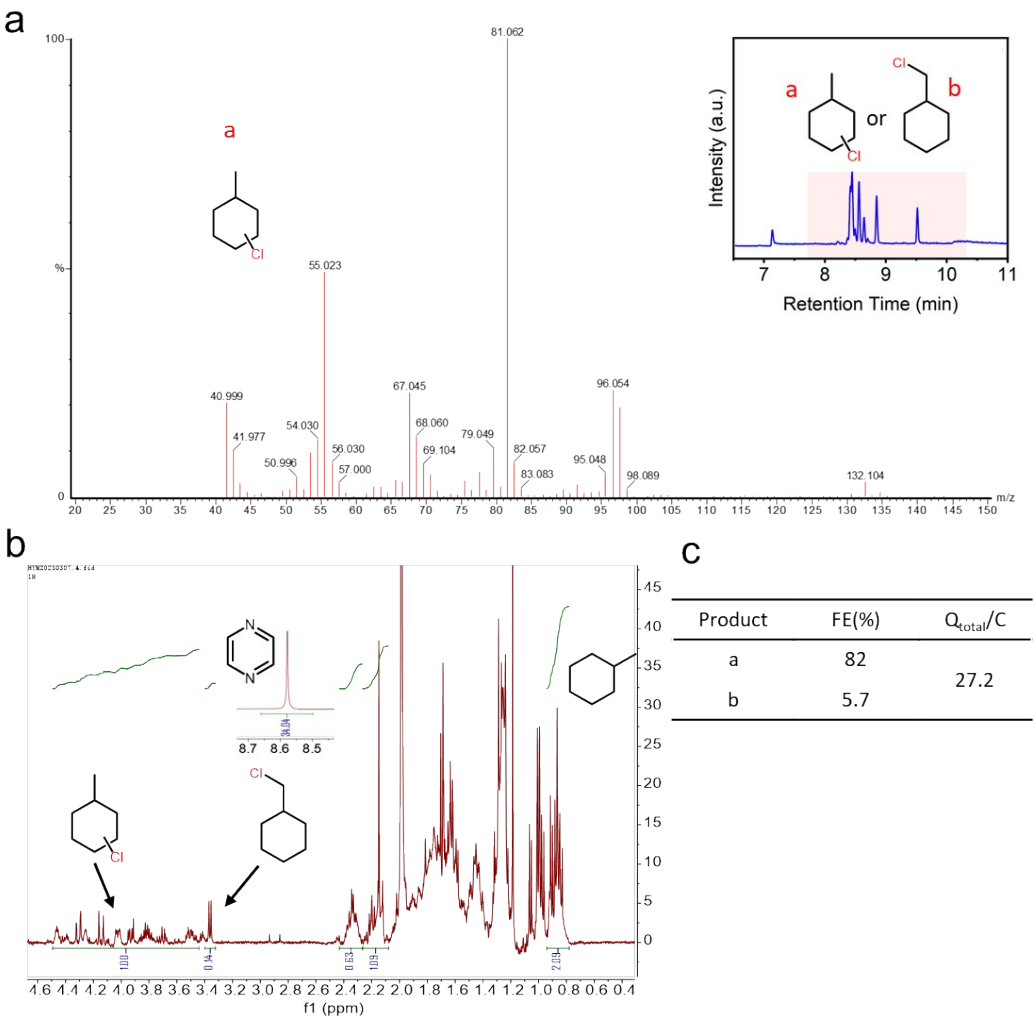

Product	FE(%)	Q_{total}/C
a	82	27.2
b	5.7	

Figure S15. (a) MS spectrum of the main chlorination product for methylcyclohexane. Insert: GC spectrum of the chlorination products for methylcyclohexane. (b) ^{1}H NMR spectrum of the chlorination products with 1 mmol pyrazine as internal standard in $CDCl_3$. (c) The calculated FE of the reaction products.

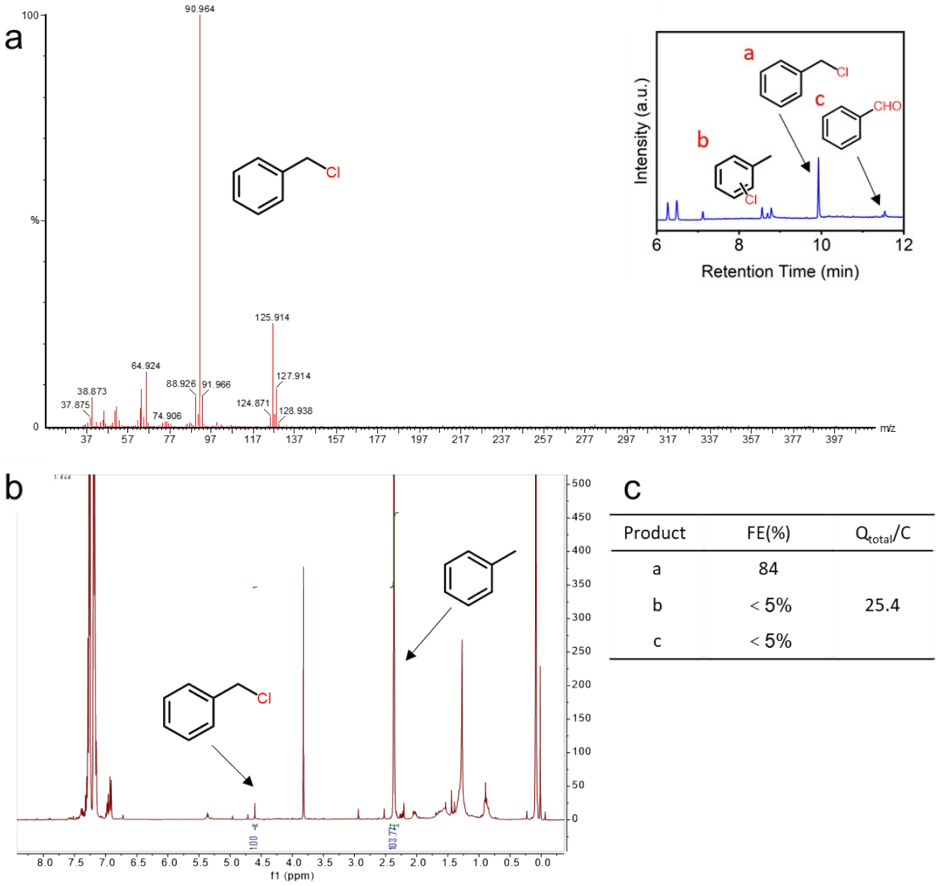

Product	FE(%)	Q_{total}/C
a	84	
b	< 5%	25.4
c	< 5%	

Figure S16. (a) MS spectrum of the main chlorination product for toluene. Insert: GC spectrum of the chlorination products for toluene. (b) ^{1}H NMR spectrum of the chlorination products in $CDCl_3$. The quantification of the minor product chlorotoluene failed due to the overlap with peaks of toluene. The amount of benzyl chloride was calculated by ratios of peak area between benzyl chloride and toluene. (c) The calculated FE of the reaction products.

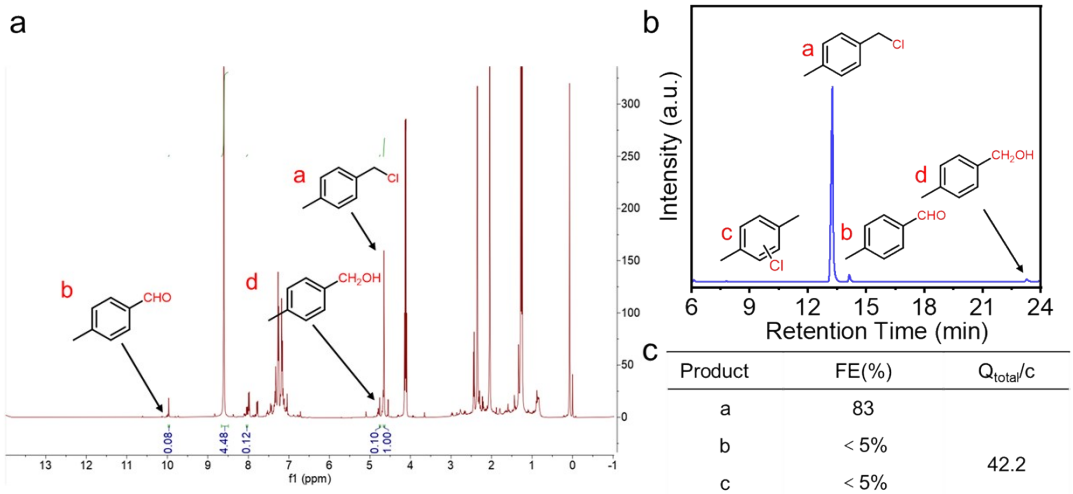

Product	FE(%)	Q_{total}/c
a	83	42.2
b	< 5%	
c	< 5%	
d	< 5%	

Figure S17. (a) ^{1}H NMR spectrum of the chlorination products in $CDCl_3$. (b) GC spectrum of the chlorination products for para-xylene. (c) The calculated FE of the reaction products. Due to the low boiling point of the products, some products may be lost during the rotary evaporation process, resulting in inaccurate ^{1}H NMR results. Therefore, products were quantified by GC.

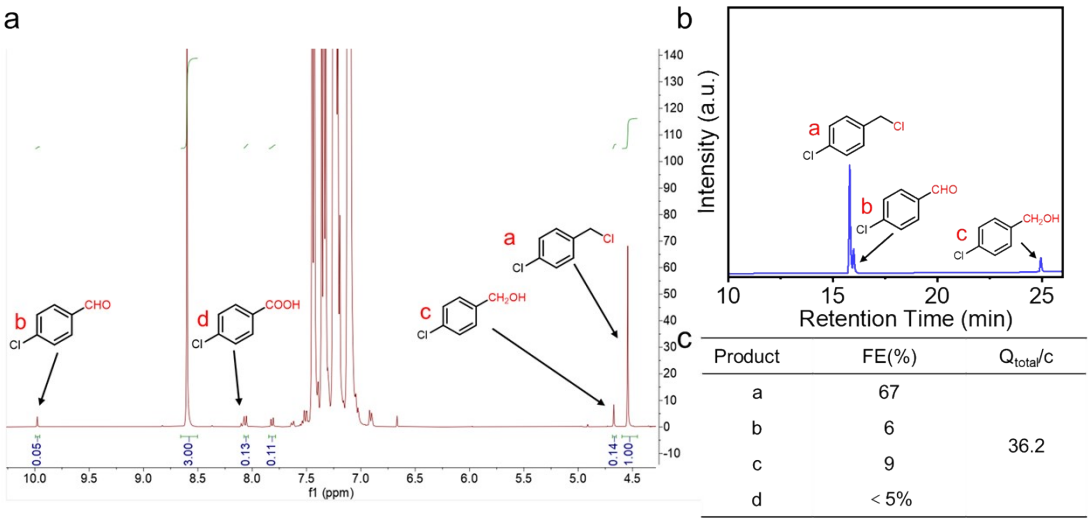

Product	FE(%)	Q_{total}/c
a	67	36.2
b	6	
c	9	
d	< 5%	

Figure S18. (a) ^{1}H NMR spectrum of the chlorination products for 4-chlorotoluene in $CDCl_3$. (b) GC spectrum of the chlorination products for 4-chlorotoluene. (c) The calculated FE of the reaction products.

a

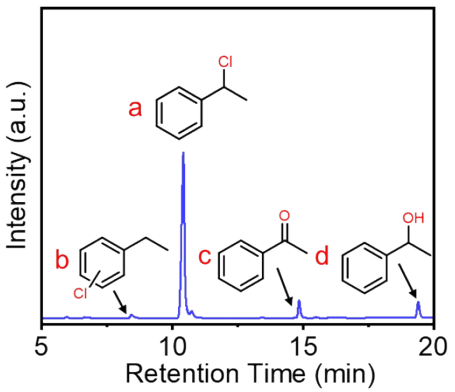

b

Product	FE(%)	Q_{total}/c
a	90	30.7
b	< 5%	
c	< 5%	
d	< 5%	

Figure S19. (a) GC spectrum of the chlorination products for ethylbenzene. (b) The calculated FE of the reaction products. Due to the low boiling point of the products, some products may be lost during the rotary evaporation process, resulting in inaccurate ^{1}H NMR results. Therefore, products were quantified by GC.

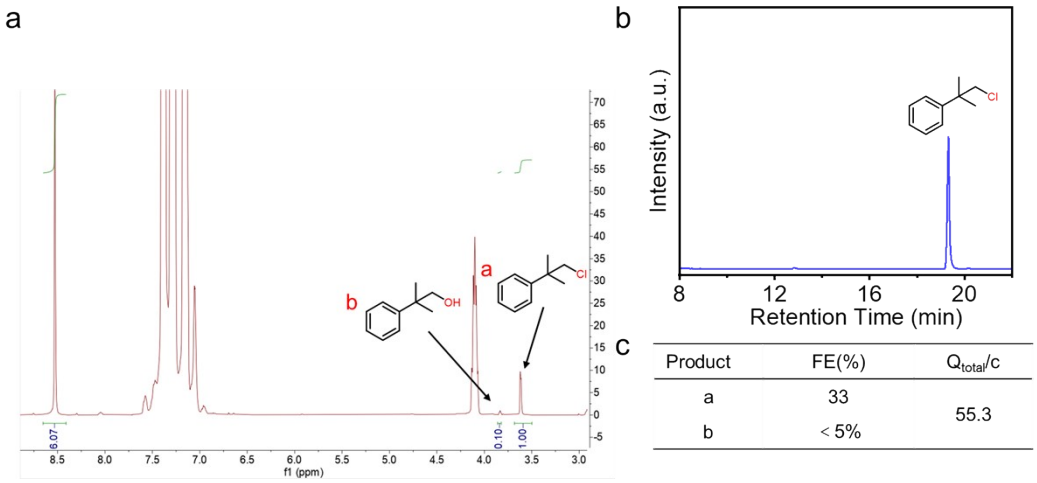

Product	FE(%)	Q_{total}/c
a	33	55.3
b	< 5%	

Figure S20. (a) ^{1}H NMR spectrum of the chlorination products for tert-butylbenzene in $CDCl_3$. (b) GC spectrum of the main chlorination products for tert-butylbenzene. (c) The calculated FE of the reaction products.

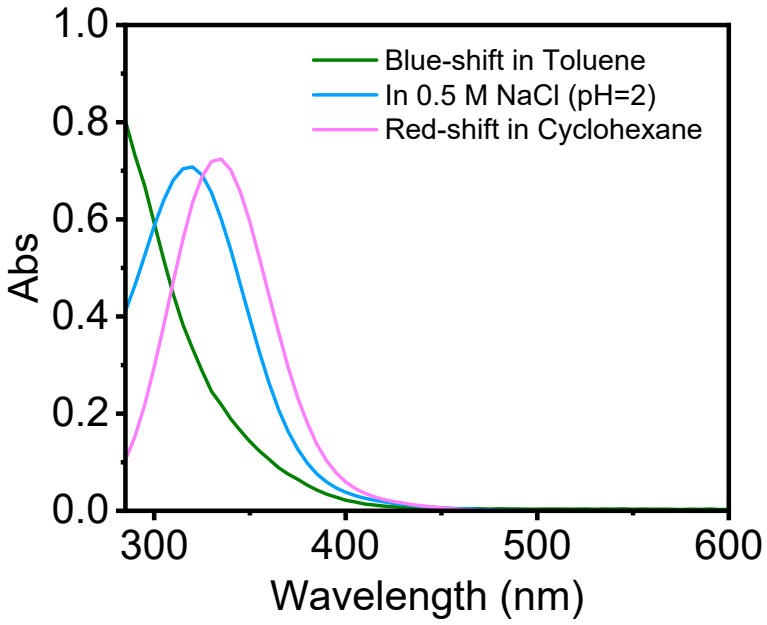

Figure S21. Absorption spectra of Cl_2 in toluene (blue-shift), in 0.5 M NaCl (pH = 2) aqueous solution and in cyclohexane (red-shift).

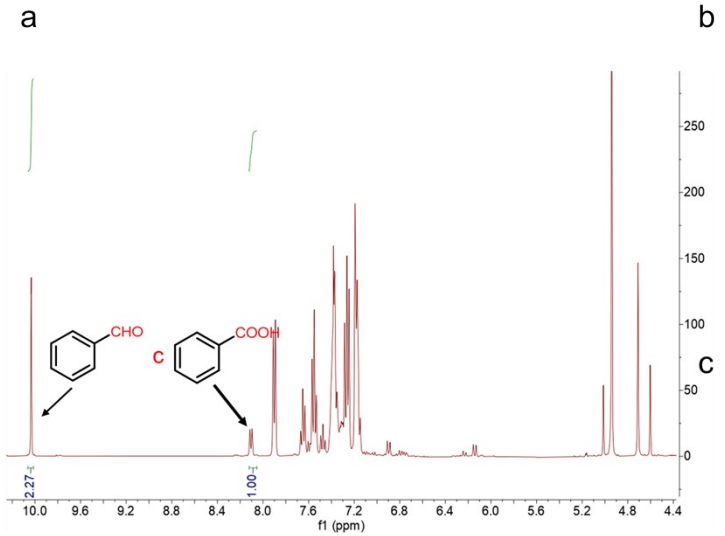

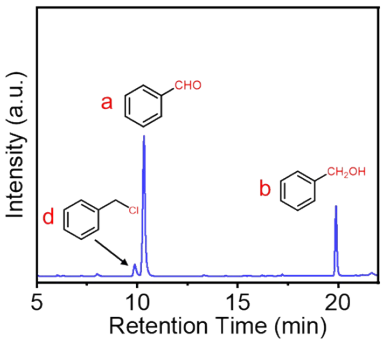

c

Product	Selectivity(%)	FE(%)
a	65	71
b	22	12
c	8	13
d	< 5%	

Figure S22. (a) ^{1}H NMR spectrum of the oxygenated products in $CDCl_3$. (b) GC spectrum of the main oxygenated products for toluene. (c) The calculated FE of the reaction products. Due to the low boiling point of the products, some products may be lost during the rotary evaporation process, resulting in inaccurate ^{1}H NMR results. Therefore, products were quantified by GC.

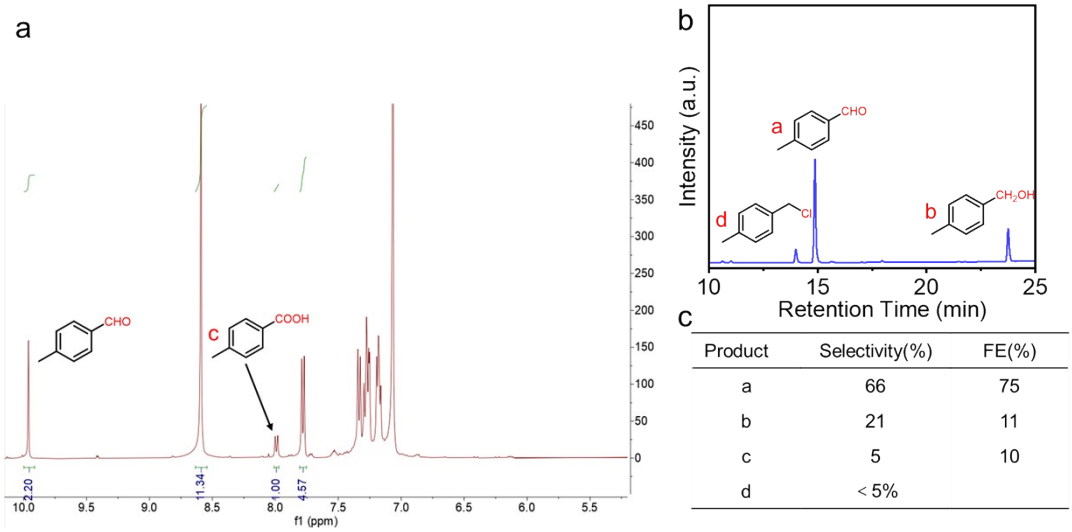

c

Product	Selectivity(%)	FE(%)
a	66	75
b	21	11
c	5	10
d	< 5%	

Figure S23. (a) ^{1}H NMR spectrum of the oxygenated products in $CDCl_3$. (b) GC spectrum of the main oxygenated products for para-xylene. (c) The calculated FE of the reaction products (quantified by GC).

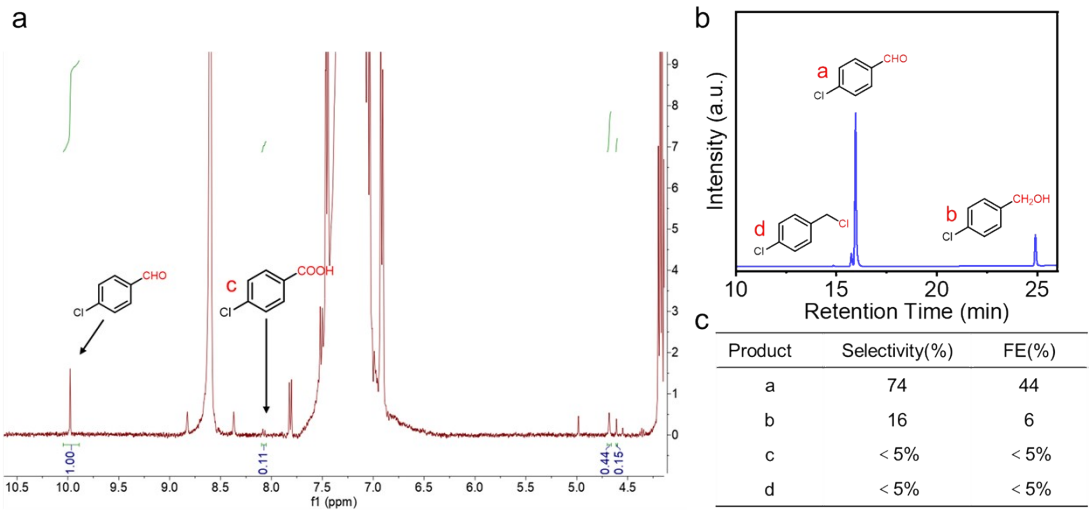

Product	Selectivity(%)	FE(%)
a	74	44
b	16	6
c	< 5%	< 5%
d	< 5%	< 5%

Figure S24. (a) ^{1}H NMR spectrum of the oxygenated products for 4-chlorotoluene in $CDCl_3$. (b) GC spectrum of the main oxygenated products for 4-chlorotoluene. (c) The calculated FE of the reaction products.

a

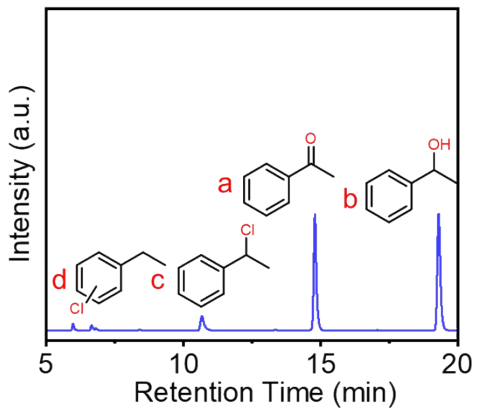

b

Product	Selectivity(%)	FE(%)
a	36	47
b	58	38
c	5	3
d	< 5%	

Figure S25. (a) GC spectrum of the main oxygenated products for ethylbenzene. (b) The calculated FE of the reaction products.

a

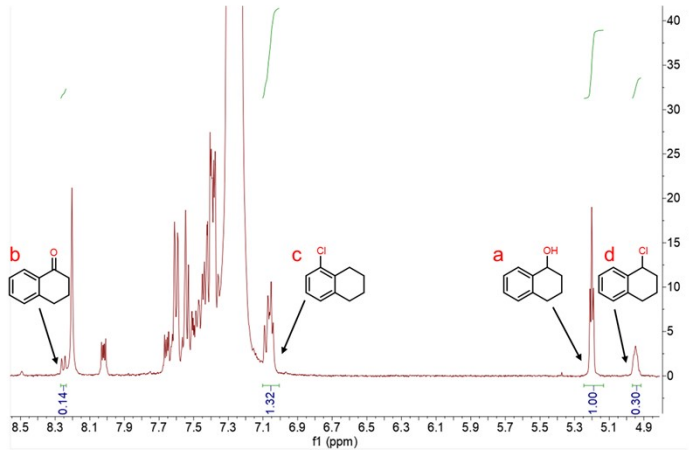

b

Product	Selectivity(%)	FE(%)
a	53	48
b	7	12
c	23	21
d	16	13

Figure S26. (a) ^{1}H NMR spectrum of the oxygenated products for tetralin in $CDCl_3$ after determined by GC-MS. (b) The calculated FE of the reaction products.

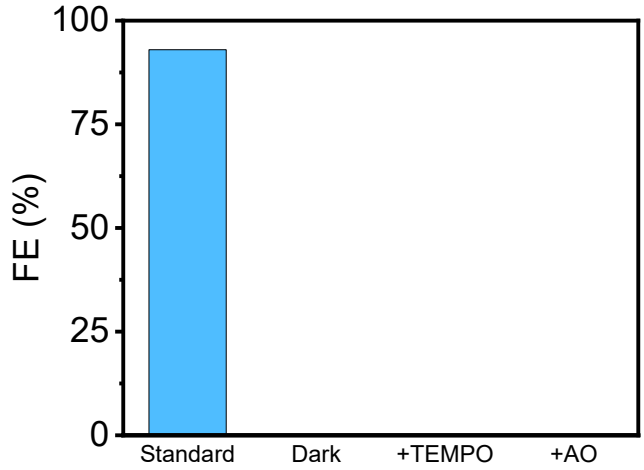

Figure S27. The FE of chlorocyclohexane production for the chlorination of cyclohexane under different conditions. Standard condition: 30 mL 0.5 M NaCl (pH = 2) aqueous solution, 2 mL cyclohexane, Ar atmosphere, 0.8 V *vs* RHE, AM 1.5G illumination (100 $mW \cdot cm^{-2}$). Dark: without illumination; +TEMPO: with 20 mM TEMPO in electrolyte; +AO: with 20 mM ammonium oxalate in electrolyte.

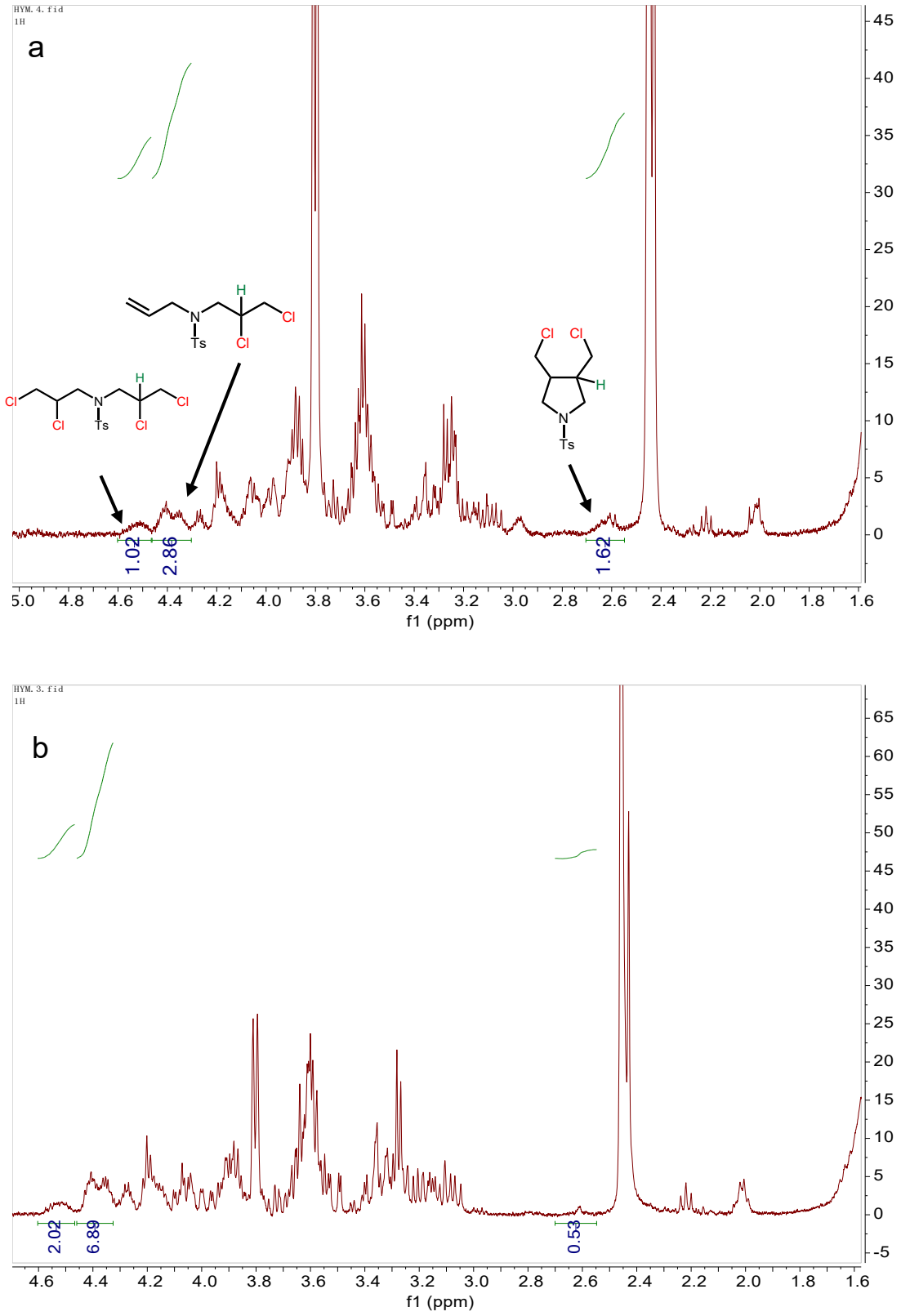

Figure S28. The ^{1}H NMR spectra of the chlorination product for **1a** in $CDCl_3$. (a) with a gap; (b) no gap.

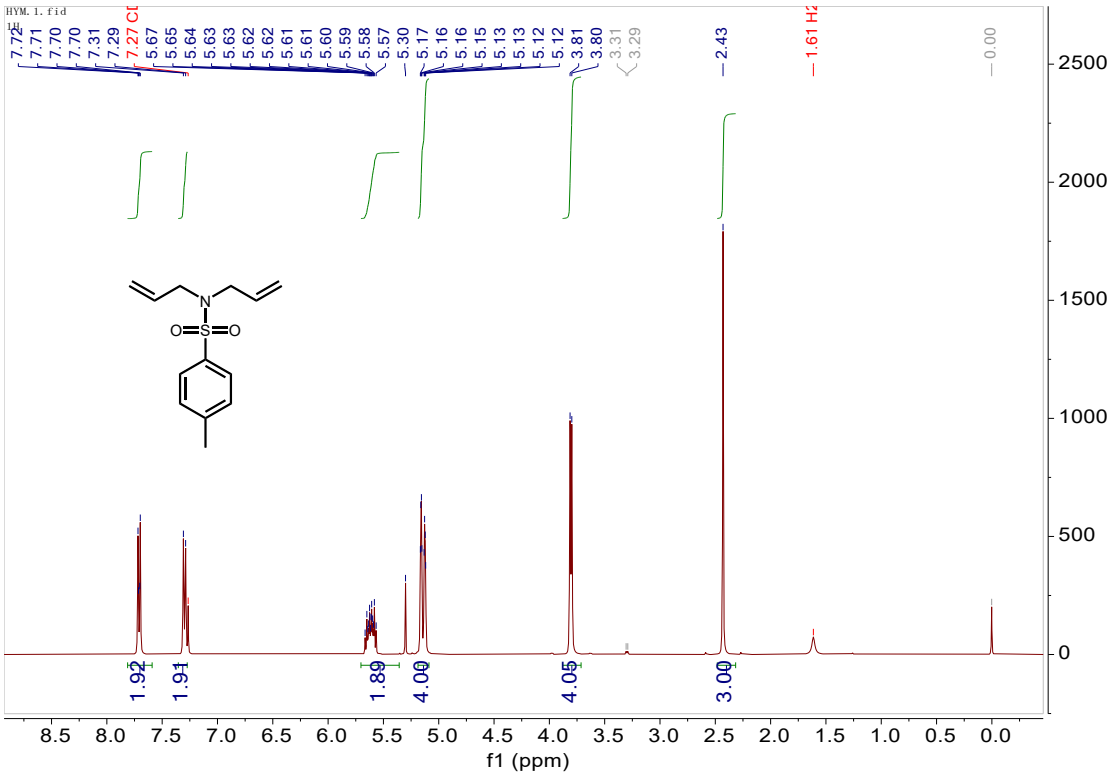

Figure S29. ^{1}H NMR spectrum of the diene **1a** in $CDCl_3$**.**

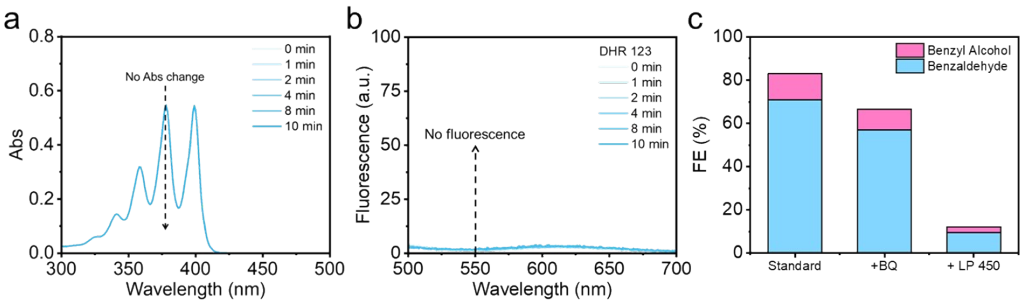

Figure S30. (a) Absorption spectra of ABDA (used as a $^1O_2$ probe, 100 μM) observed in 0.1 M NaCl (pH = 2) aqueous solution in an operating PEC cell with different reaction times. (b) Superoxide anion ($O_2^{\bullet-}$) detection using the dihydrorhodamine 123 (DHRl23) assay. (c) Quenching experiment of $O_2^{\bullet-}$ with BQ as a scavenger and $Cl^{\bullet}$ with long-pass filter (λ > 405 nm).

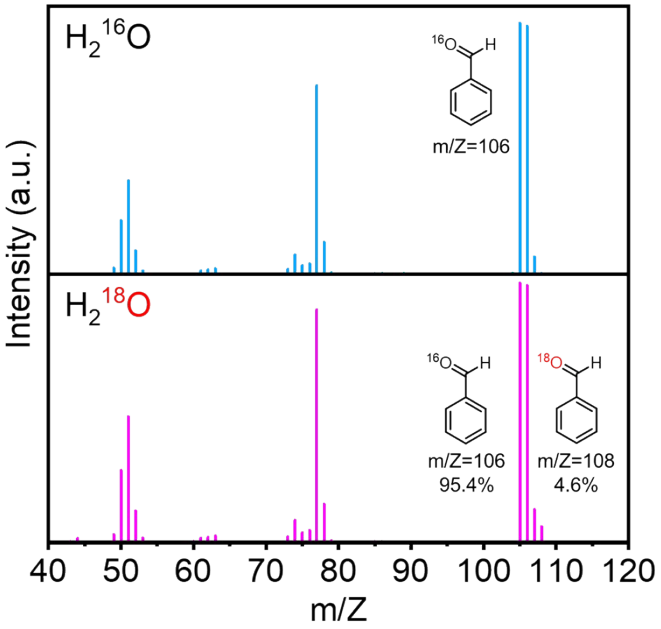

Figure S31. Mass spectra of the benzaldehyde in the isotope tracing experiments of $H_2{}^{16}O$ and $H_2{}^{18}O$. Proportions of the isotope labeled products are marked in the figure, calculated by the intensity of fragment peaks.

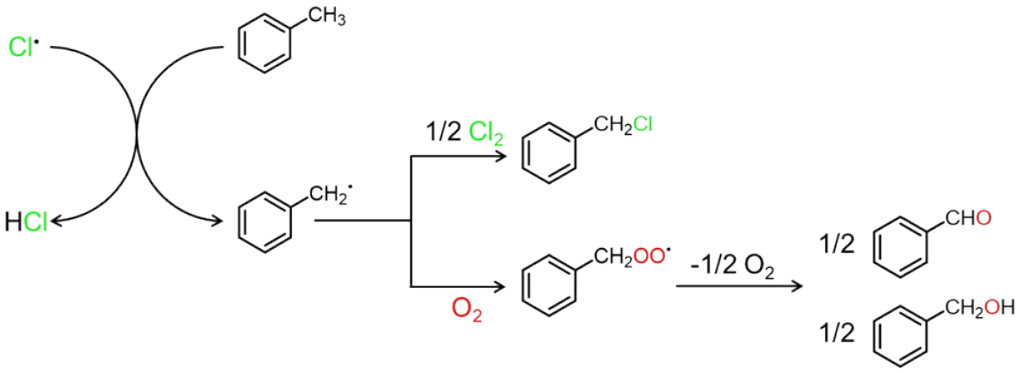

Figure S32. Hypothesis of the chlorination and oxygenation reaction driven by Cl•.

After Cl_2 is generated via the PEC process, it undergoes photolysis to produce Cl•. These radicals perform hydrogen atom transfer (HAT) with the substrate's C-H bond, forming a carbon-centered radical and HCl. Under an Ar atmosphere, the carbon centered radical reacts with Cl_2 to yield chlorinated products. In contrast, under an O_2 atmosphere, the radical is more likely captured by O_2 due to the higher O_2 concentration in the solvent to afford an organic superoxide intermediate. Subsequent electron and proton transfer, followed by O-O bond cleavage, lead to the formation of oxygenated products.[6]

Table S1-S4

Table S1. The relative amounts of various elements of $BiVO_4/TiO_2/CoNi_2O_x$ from the STEM-EDS analysis.

Element	Wt (%)	Wt (%) SD	Atomic (%)
O	17.11	0.28	60.72
Ti	0.39	0.05	0.46
V	14.90	0.13	16.61
Co	1.86	0.06	1.79
Ni	3.70	0.08	3.57
Bi	62.04	0.27	16.85
Total	100.00		100.00

Table S2. η_{ct} values of different photoanodes calculated from IMPS results.

Photoanode	η_{ct} (%)
$BiVO_4$	0.53
$BiVO_4/CoNi_2O_x$	0.62
$BiVO_4/TiO_2$	0.75
$BiVO_4/TiO_2/CoNi_2O_x$	0.95

Table S3. The R_{ct}, experimental errors and χ^2 (chi-squared) values calculated from EIS results for different anodes.

Photoanode	R_{ct} (Ω)	Experimental Errors	χ^2
$BiVO_4$	4229	0.47%	0.000308
$BiVO_4/CoNi_2O_x$	1864	0.64%	0.000485
$BiVO_4/TiO_2$	2785	0.73%	0.000928
$BiVO_4/TiO_2/CoNi_2O_x$	907	0.69%	0.000945

Table S4: Optimization of the two-step coupled PEC chlorination reaction conditions.

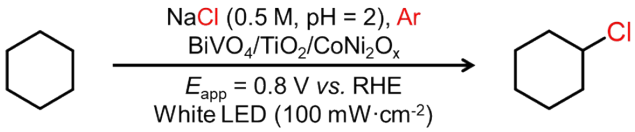

Entry	Condition	Yield(%)
1	Standard conditions[a]	93
2	No PEC step (Na_2SO_4 instead of NaCl)	n.d.
3	No PEC step (no E_{app})[b]	n.d.
4	No PC step (Cl_2 not exposed to light)[c]	n.d.
5	PC step only (Cl_2 introduced externally)[d]	52

[a] Standard reaction conditions: 30 ml of 0.5 M NaCl (pH = 2) solution, 0.15 mmol cyclohexane, $BiVO_4/TiO_2/CoNi_2O_x$, 0.8 V vs RHE, white LED (100 mW/cm^2), 1 atm Ar.

[b] No PEC step (no E_{app}): No electrical bias was applied under white light irradiation.

[c] No PC step: Cl_2 was prevented from being excited by light using the setup shown in Figure 5b.

[d] PC step only: No E_{app}; Cl_2-saturated 0.5 M NaCl (pH = 2) aqueous solution with white light irradiation. The yield was significantly lower, likely due to the inability of Cl_2 to regenerate in the absence of the PEC process.

References

1. D. Liu, J.-C. Liu, W. Cai, J. Ma, H. B. Yang, H. Xiao, J. Li, Y. Xiong, Y. Huang and B. Liu, *Nat. Commun.*, 2019, **10**, 1779.
2. Q. Wang, T. Li, C. Yang, M. Chen, A. Guan, L. Yang, S. Li, X. Lv, Y. Wang and G. Zheng, *Angew. Chem. Int. Ed.*, 2021, **60**, 17398-17403.
3. E. A. Ponomarev and L. M. Peter, *J. Electroanal. Chem.*, 1995, **396**, 219-226.
4. N. Fu, G. S. Sauer and S. Lin, *J. Am. Chem. Soc.*, 2017, **139**, 15548-15553.
5. D. Yu, R. Ji, Z. Sun, W. Li and Z.-Q. Liu, *Tetrahedron Lett.*, 2021, **86**, 153514.
6. Y. Itabashi, H. Asahara and K. Ohkubo, *Chem. Commun.*, 2023, **59**, 7506-7517.